Synthesis and Performance of Nb^{5+}-Doped $LiFePO_4$/C as Cathode Material in Lithium-Ion Battery

Aili Zhang, Axiang Li, Jili Xia, Zhongcai Shao[*]

School of Environment and Chemical Engineering, Shenyang Ligong University
[*]E-mail: 1764748131@qq.com

Nb^{5+}-doped $LiFePO_4$/C was synthesized as the cathode material by carbon-thermal reduction method in lithium-ion battery. The XRD, SEM, charge and discharge cycles and cycling performance tests were used to study the crystal structure, surface morphology and electrochemical properties of $LiFe_{1-x}Nb_xPO_4$/C. The effects of different synthesis conditions on $LiFe_{1-x}Nb_xPO_4$/C cathode materials were discussed systematically. Finally, the optimal raw materials and process parameters were determined to synthesize $LiFe_{1-x}Nb_xPO_4$/C cathode material with better performance. The electrochemical properties results showed that $LiFe_{1-x}Nb_xPO_4$/C (x=0.02) had good electrochemical capacity at 0.1C rate, which also had the highest charge-discharge capacity, good high-rate performance and small attenuation. And the discharge specific capacity reached 146.881 mAh·g^{-1} at 0.1C rate, which was increased by 11.18% than 132.108 mAh·g^{-1} of the initial discharge specific capacity without doping Nb^{5+}. After 20 cycles, the charge-discharge specific capacity was almost unchanged and charge and discharge at different rates also showed good stability.

Keywords: $LiFePO_4$; Cathode material; Lithium-ion Battery; Doping; Performance

1. INTRODUCTION

With the development of science and technology, lithium-ion battery has been gradually applied in the field of power and energy storage battery [1-2]. $LiFePO_4$ is used as preferred cathode material of large capacity battery because lithium-ion battery produced with $LiFePO_4$ has good thermal stability and long cycle life [3-5]. $LiFePO_4$ attracted people's attention because of high discharge capacity, low cost, rich source of raw materials, environmentally friendly, high safety performance and other advantages [6]. However, $LiFePO_4$ material also has its own some major drawbacks, which are lithium-ion diffusion coefficient, low electronic conductivity rate, low material temperature and poor electrochemical properties at high rate charge and discharge [7-9]. These become main problem to

restrict wide use of $LiFePO_4$ material. At present, the methods for modifying $LiFePO_4$ materials mainly include coating conductive materials such as carbon and metal oxides on the surface of $LiFePO_4$ particles, doping metal ions into $LiFePO_4$ crystals, and refining $LiFePO_4$ particle size [10-11]. Ion doping is an important means to improve performance of cathode material of Li-ion battery. $LiFePO_4$ is a semiconductor with a forbidden band width of about 0.3eV. Un-doped $LiFePO_4$ is an n-type semiconductor with an activation energy close to 500eV. While doped $LiFePO_4$ is a p-type semiconductor, of which activation energy reduces to 60~80eV. Reduction of activation energy is good for the electronic transition, which can enhance the electronic conductivity of the material [12]. The conductivity of the doped material can be increased by 8 orders of magnitude. By doping, the lattice of the $LiFePO_4$ material can form many holes and change the Fermi level of the material to improve the conductivity of the material [13-14].

The main research was modification of $LiFePO_4/C$ cathode material by doping Nb^{5+} in this paper. Through a series of performance tests, the test results were analyzed to study the impact of doping Nb^{5+} on the physical and electrochemical properties of the composite material to determine the optimal doping amount of Nb^{5+}.

2. EXPERIMENT

$LiFe_{1-x}Nb_xPO_4/C$ with doping Nb^{5+} was synthesized by carbon-thermal reduction method. The experiment used $LiOH·H_2O$ as the lithium source, Fe_2O_3 as the iron source, $NH_4H_2PO_4$ as the phosphorus source, tartaric acid ($C_4H_6O_6$) as the carbon source and Nb_2O_5 as Nb source. According to the elemental molar ratio of Li: Fe: Nb: P= 1.05: (1-x): x:1(x=0.01, 0.02, 0.03) to weigh the drugs and place them in an agate mortar for grinding. Then grind them thoroughly into the beaker and add ethanol to stir. The sample was placed in a bench-top oven at 85°C after 1h. The dried sample was well ground into in a crucible. Finally, it was placed in a vacuum tube-type high-temperature sintering furnace and calcined at 350°C for 4h in a nitrogen atmosphere and then heated at 750°C (700°C, 800°C, 850°C) for 6h (5h, 7h, 8h) to prepare Nb^{5+}-doped $LiFe_{1-x}Nb_xPO_4/C$. The target samples $LiFe_{0.98}Nb_{0.02}PO_4/C$, $LiFe_{0.96}Nb_{0.04}PO_4/C$ and $LiFe_{0.94}Nb_{0.06}PO_4/C$ can be prepared separately.

The prepared $LiFe_{1-x}Nb_xPO_4/C$ and conductive agent acetylene black and binder PVDF were mixed in ratio of 80:10:10. After mixing them, an appropriate amount of N-methyl pyrrolidone slurry was added. Magnetic stirring for a certain time was used to mix evenly to coat aluminum foil. Then dry the sample naturally. The cathode material film cut into wafers, and then placed in a vacuum to dry at 80°C for 10 hours and weighed. The weighed piece, the simulated battery case and the current collector were placed into a vacuum oven at 80°C for 8 hours, which can be used to make anode piece of assembled battery. Using lithium metal as cathode electrode, polypropylene microporous membrane as separator material and Ethylene carbonate, dimethyl carbonate, and ethyl methyl carbonate mixed in a ratio of 1: 1: 1 to prepare an electrolyte solution of $LiPF_6$, and then assembled into a two-electrode analog battery in a glove box. Finally, test charge-discharge specific capacity and cycle performance of the cathode material by using multi-channel battery programmable controller at room temperature.

Phase analysis of $LiFe_{1-x}Nb_xPO_4$/C powder was carried out by using X-ray diffractometer (D/Max-2200, Rigaku, Japan), in which Cu Kα target was used. The surface morphology of $LiFe_{1-x}Nb_xPO_4$/C powder was analyzed and characterized by S-4800 field emission scanning electron microscope (Japan Electronics Co. Ltd.). The new Veyron current charge and discharge meter test system (Liaoning Instrument Research Institute, China) was used to charge and discharge test at room temperature, using the voltage range of 2.5~4.2 V and charge-discharge rate of 0.1C. Using CHI660E electrochemical workstation (Shanghai Chenhua Instrument Co. Ltd.) to test the cycle performance of the material. Scanning rate was 0.1 mV/s and scanning voltage range was 2.0~4.2 V. Shanghai Chenhua CHI660E was used to test AC impedance of electrode materials. The test was conducted under an open circuit voltage. The scanning range was 100kHz~10mHz and the test amplitude was 5 mV.

3. RESULTS AND DISCUSSION

3.1. Crystal Structure of $LiFe_{1-X}Nb_xPO_4$/C Composites

Figure 1 shows the XRD patterns of $LiFe_{1-x}Nb_xPO_4$/C cathode material prepared with different doping amount of Nb^{5+}. It can be seen that the XRD patterns of the three samples were similar, which has strong diffraction peaks. The three samples are consistent with the standard $LiFePO_4$ spectra, indicating that they all have olivine structure. The Diffraction peaks can be indexed by an orthorhombic Pnma structure (JCPDS 83-2092), which are similar to the previous reports [15,16,19]. The addition of Nb^{5+} does not 2change the crystal structure of $LiFePO_4$/C but makes it good crystallinity. Compared with $LiFePO_4$/C cathode material without doping Nb^{5+}, the crystallinity is higher and the diffraction peak intensity is bigger and sharper. However, when the doping amount was too high, perhaps the structure of the synthetic $LiFe_{1-x}Nb_xPO_4$/C would be different, and exhibited some unpleasant results. A comprehensive comparison of the diffraction peaks of the three samples shows that the crystal properties of the samples were best when the doping amount of Nb^{5+} is 0.02.
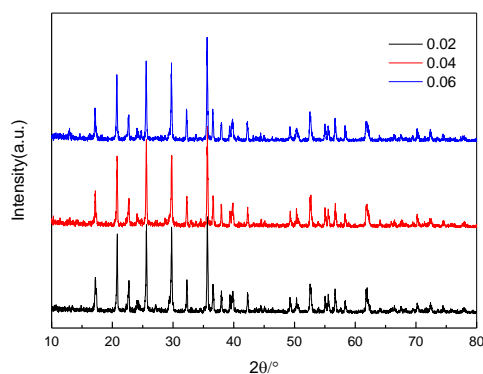

Figure 1. XRD of $LiFe_{1-X}Nb_xPO_4$/C (x=0.01, 0.02, 0.03) with different Nb^{5+} doping amount

3.2. The Surface Morphology of LiFe$_{1-X}$Nb$_x$PO$_4$/C Composites

Figure 2, SEM images of LiFe$_{1-x}$Nb$_x$PO$_4$/C with different Nb^{5+} doping amount. A$_1$, A$_2$, A$_3$ represent Nb^{5+} doping amount of 0.01, 0.02 and 0.03, respectively. As can be seen from the figure, the sample after doping Nb^{5+}, the particle size is significantly refined. It seems that the addition of Nb^{5+} plays an important role in inhibiting particle growth. Among them, when the doping amount is 0.02, the particle size is small and dispersed uniformly. And the specific surface area of the material is large, which can effectively improve the diffusion path of Li$^+$. When the doping amount is 0.01, difference of the particle size is very large and uneven. When the doping amount is 0.03, the particle size is not uniform and agglomeration phenomenon is very severe. Particle refinement is good for increasing Li$^+$ diffusion rate to improve the electrochemical properties of the material. It is also beneficial for electrolyte to contact the cathode material, which can enhance the electrochemical performance of the samples. LiFe$_{1-x}$Nb$_x$PO$_4$/C with 0.02 Nb^{5+} doping exhibited better electrochemical performance.

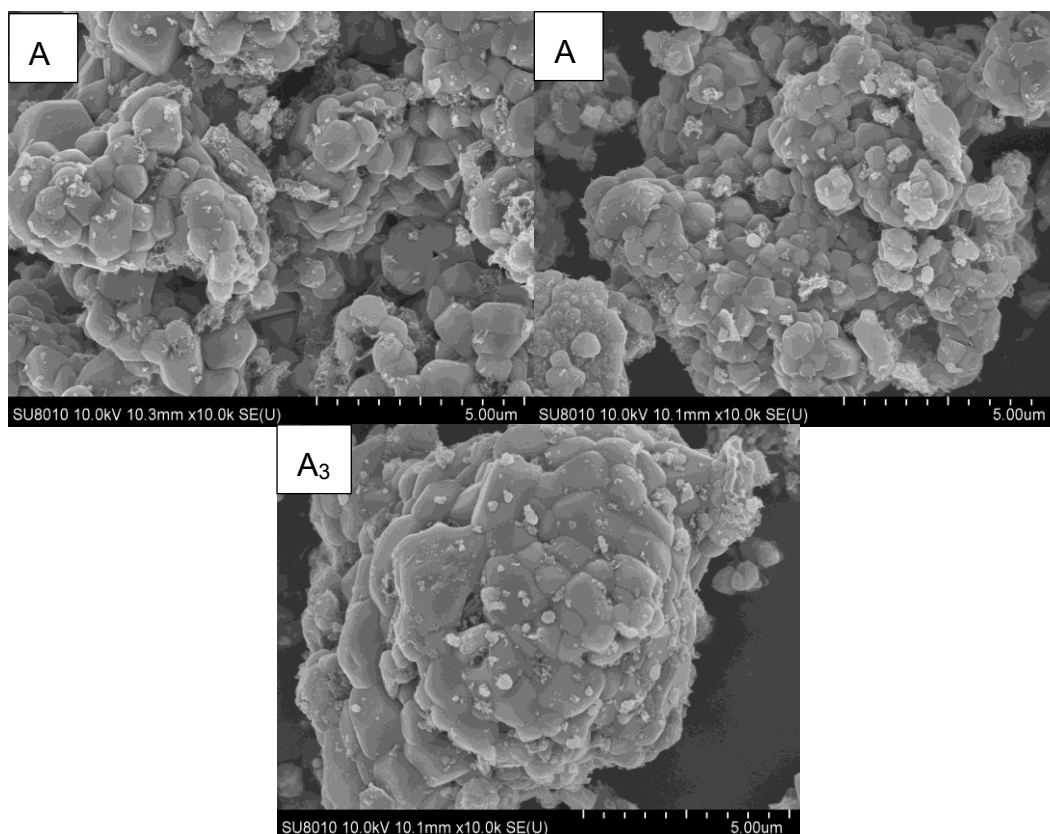**Figure 2.** SEM of LiFe$_{1-X}$Nb$_x$PO$_4$/C (x=0.01, 0.02, 0.03) with different Nb^{5+} doping amount

3.3. The Charge and Discharge Properties of LiFe$_{1-X}$Nb$_x$PO$_4$/C Composites

Figure 3 shows the first charge and discharge curves of LiFe$_{1-x}$Nb$_x$PO$_4$/C (x=0.01, 0.02, 0.03) samples at different magnifications.

The specific discharge capacity of $LiFePO_4$/C of un-doped Nb^{5+} is 136.385 mAh·g^{-1}, and the initial charge-discharge capacity of the sample is increased compared with the Nb^{5+}-doped material. The first discharge capacities of $LiFe_{1-x}Nb_xPO_4$/C (x=0.01, 0.02, 0.03) are 146.881 mAh·g^{-1}, 142.925 mAh·g^{-1} and 139.656 mAh·g^{-1}, respectively.
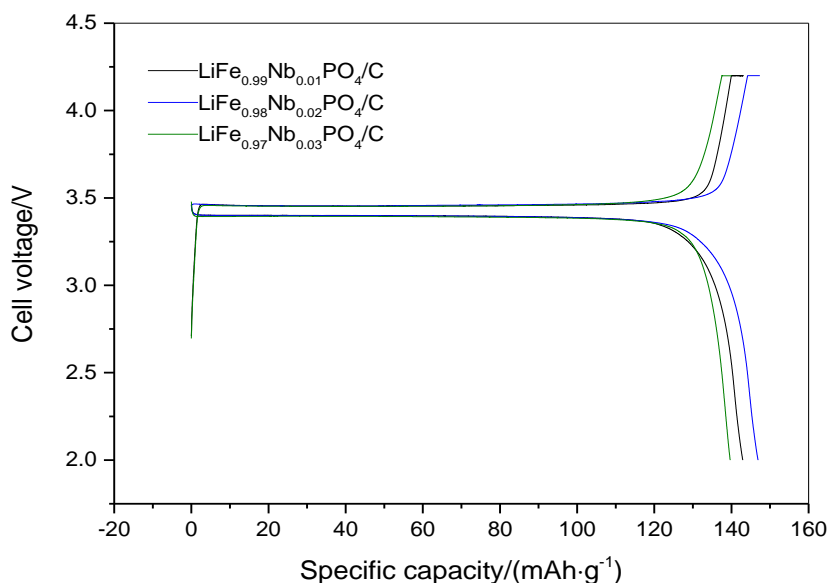

Figure 3. Initial charge-discharge curve of $LiFe_{1-x}Nb_xPO_4$/C (x=0.01, 0.02, 0.03) at different magnifications

It can be seen that the charge and discharge voltage of the samples platform are longer and more stable. The degree of polarization decreases after doping Nb^{5+}. $LiFe_{1-x}Nb_xPO_4$/C (x=0.01, 0.02, 0.03) has better electrochemical performance. In addition, the curves of charging process and discharging process are almost the same, which shows that the oxidation and reduction reactions of Nb^{5+}-doped materials have good reversibility. It makes the material have better cycling performance. When the doping amount is 0.01 and 0.02, the specific discharge capacity increases gradually. The doping of Nb^{5+} can not only facilitate the oxidation of Fe^{3+}/Fe^{2+} to a certain degree but also provide some of the electricity. It is conducive to the increase of specific capacity. However, when the doping amount is 0.03, the specific discharge capacity decreases due to the ion radius of 0.078 nm and 0.076 nm for Fe^{2+} and Li^+, respectively, and the ion radius of Nb^{3+} is 0.072 nm. The radius of Nb^{3+} is smaller than that of Fe^{2+} and Li^+. When Nb^{5+} occupies Fe sites, Li^+ "holes" are formed, and the lattice shrinks, causing the diffusion path of Li^+ to be reduced. However, when reaching a certain level, the excessive reduction of the lattice will not be conducive to the embedding of Li^+, so that this negative influence will be the main factor to cause that the discharge specific capacity decreases. After Nb^{5+} ion doping, the improvement in discharge capacity and cycling performance are confirmed by the experiment results presented here. It has been claimed that the conductivity of p-type semiconductor may be improved via a dopant effect [17]. Among them, material has the highest discharge capacity when x is equal to 0.02. Therefore, the electrochemical performance of $LiFe_{0.98}Nb_{0.02}PO_4$/C is better.

3.4. Cycle Performance and Rate Performance of LiFe₁₋ₓNbₓPO₄/C Composites

3.4. Cycle Performance and Rate Performance of LiFe$_{1-X}$Nb$_x$PO$_4$/C Composites

Figure 4 shows the cycle performance and first charge-discharge curve of LiFe$_{1-x}$Nb$_x$PO$_4$/C (x=0.01, 0.02, 0.03) at different magnifications.

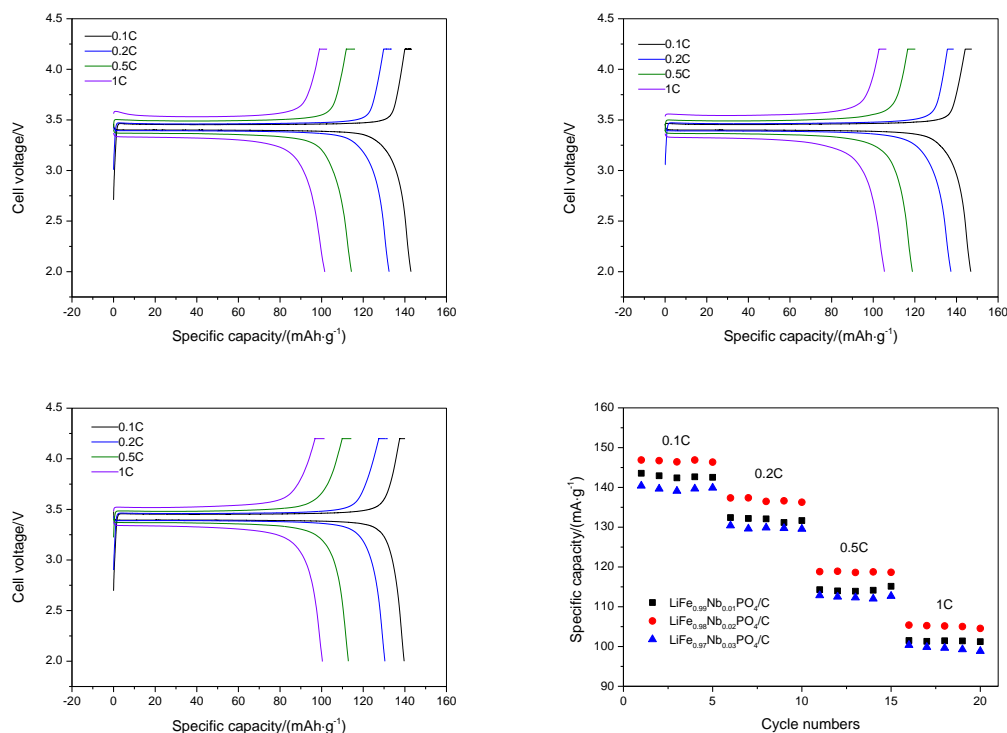**Figure 4.** Cycling performance and the first charge and discharge curve of LiFe$_{1-x}$Nb$_x$PO$_4$/C (x=0.01, 0.02, 0.03) at different rates

The discharge capacities of LiFe$_{1-x}$Nb$_x$PO$_4$/C (x=0.01, 0.02, 0.03) are 132.421 mAh·g^{-1}, 137.351 mAh·g^{-1} and 130.406 mAh·g^{-1} at 0.2C discharge rate, respectively. Compared with 0.1C, the specific discharge capacity decreased by 7.8%, 6.5% and 7.1%, respectively. LiFe$_{0.98}$Nb$_{0.02}$PO$_4$/C is more suitable for larger current than the other two materials. However, the specific discharge capacity decreased by 13.7%, 13.5% and 13.5% when the discharge rate increased to 0.5C. When the discharge rate increased to 1C, the specific discharge capacity decreased by 11.2%, 11.3% and 11.1%, respectively. Thereby, the rate performance of our Nb^{5+} doped LiFe$_{1-x}$Nb$_x$PO$_4$/C material was close to V-doped LiFe$_{1-x}$V$_x$PO$_4$/C [18], which exhibited the better rate performance among the various ions doped LiFePO$_4$/C materials in the literature [12]. It can be seen that the amount of reduction of the three materials is almost the same, indicating that when the large current discharge, the amount of doping has little effect on the material at a large rate of discharge. But LiFe$_{0.98}$Nb$_{0.02}$PO$_4$/C material always has a larger discharge capacity. It can be seen from the cycle performance diagram that the three materials have better cycle performance, good reversibility and lower decay rate. The rate performance of LiFe$_{0.98}$Nb$_{0.02}$PO$_4$/C cathode material could be attributed to the enhancement of the electronic conductivity and diffusion of Li$^+$ after doping Nb^{5+}, and also to the high stability of the

olivine structure and the minor adjustments of lattice structure upon cycling [19]. Compared with the other two materials, $LiFe_{0.98}Nb_{0.02}PO_4/C$ has a higher specific discharge capacity at different discharge rates. The capacity retention rate was up to 98.8% after 20 cycles. In addition, the reversibility is better, showing better electrochemical performance.

Yang [12] synthesized Ni-doped $LiFe_{0.98}Ni_{0.02}PO_4/C$ composites to study the electrochemical properties by solid-state synthesis method. The results showed discharge capacity of $LiFe_{0.98}Ni_{0.02}PO_4/C$ reached 154.7 mAh g^{-1} (at 0.2C rate). The capacity retention rate was 98.8% after 30 cycles.

Shao [18] via carbon-thermal reduction method prepared $LiFe_{0.96}V_{0.04}PO_4/C$ doping with V^{5+}. We can found that discharge capacity of $LiFe_{0.96}V_{0.04}PO_4/C$ reached 141.1 mAh g^{-1} at 0.1C, after 20 cycles, the capacity retention rate was 97.0%.

Meng [19] studied electrochemical properties of Sm-doped $LiFePO_4/C$ by a sol-gel method. The experimental results showed $LiFe_{0.94}Sm_{0.06}PO_4/C$ had better discharge capacities of about 162.1 mAhg^{-1} at a rate of 0.1C and the capacity retention rate was 97.8% after 20 cycles.

Sun [20] prepared $LiFe_{0.96}V_{0.04}PO_4/C$ doping with V^{5+} by solid state reaction. He came to the conclusion that V^{5+} has obvious effect on improving its electronic or ionic mobility. The tests demonstrated discharge capacity of $LiFe_{0.96}V_{0.04}PO_4/C$ reached 146.5 mAh g^{-1} at 0.1C. The capacity retention rate was 96.0%.

Table 1. Comparison of Different Ion Doping of $LiFePO_4/C$ on Electrochemical Properties

Different ions doping	Ions form	Discharge capacity	Capacity retention	References
$LiFe_{0.98}Ni_{0.02}PO_4/C$	Ni^{2+}	154.7	98.8%	[12]
$LiFe_{0.96}V_{0.04}PO_4/C$	V^{5+}	141.1	97.0%	[18]
$LiFe_{0.94}Sm_{0.06}PO_4/C$	Sm^{3+}	162.1	97.8%	[19]
$LiFe_{0.96}V_{0.04}PO_4/C$	V^{5+}	146.5	96.0%	[20]
$LiFe_{0.98}Nb_{0.02}PO_4/C$	Nb^{5+}	146.9	98.8%	This study

3.5. Cyclic Voltammetry of $LiFe_{1-X}Nb_xPO_4/C$ Composites

Figure 5 shows the cyclic voltammetry of synthesized samples with Nb^{5+} doping amount of 0.01, 0.02 and 0.03, respectively.
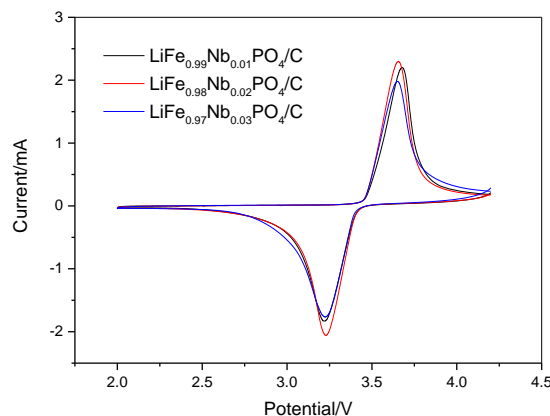
Figure 5. Cyclic voltammetry of $LiFe_{1-x}Nb_xPO_4/C$ (x=0.01, 0.02, 0.03)

The voltage range is 2.0~4.2 V and the scanning speed is 0.1 mV/s. It can be seen from the figure that a pair of redox peaks appear in the cycle corresponding to the redox reactions of Fe^{3+}/Fe^{2+} and Li^+/Li, respectively, which is consistent with the previous report [20]. In addition, as the doping amount increases, the position of the oxidation peak and the reduction peak appear offset of different degrees, but the movement is not so large. Among them, the sample synthesized at a doping amount of 0.02 has a higher peak intensity and a narrower peak shape, which is more conducive to the migration of electrons and the diffusion and insertion of Li^+ during the electrode reaction. This result may be important to practical production because it means that the addition amount of a relatively little Nb^{5+} can fully use the cathode material at a lower charge voltage [21]. Therefore, when the doping amount of Nb^{5+} is 0.02, synthesized sample has better electrochemical properties.

3.6. AC Impedance of $LiFe_{1-x}Nb_xPO_4/C$ Composites

Figure 6 is AC impedance of $LiFe_{1-x}Nb_xPO_4/C$ (x=0.01, 0.02, 0.03). The AC impedance diagrams of the three materials are composed of the intercept of the high frequency region and the x-axis, the semicircle of the high frequency region and the oblique line of the low frequency region. The starting point of the semicircle in the high frequency region is the body resistance of the battery system, including the physical resistance of the battery case, current collectors and the resistance of the separator and the electrolyte. It can be seen that the bulk resistance of the three materials is almost the same. The diameter of the semicircle in the high frequency region represents the resistance when the lithium ion through the process of the solid electrolyte membrane and the charge transfer resistance of the electrochemical reaction. The semicircular arc radius of the high frequency region can approximate the size of the impedance. The larger the radius shows the resistance is the larger. It can be seen that the impedance of descending order is $LiFe_{0.97}Nb_{0.03}PO_4/C$, $LiFe_{0.99}Nb_{0.01}PO_4/C$ and $LiFe_{0.98}Nb_{0.02}PO_4/C$. Among them, the impedance of $LiFe_{0.98}Nb_{0.02}PO_4/C$ is the lowest than other materials. The diagonal line in the low frequency region represents the diffusion impedance, which is commonly known as the Warburg impedance, formed by the diffusion of Li^+ between the electrode

surface and the electrolyte. This viewpoint is also reported in previous paper [22]. The slopes of slash of the low frequencies in the three samples are approximately the same. This shows that the difference between the impedances of the three materials during charging and discharging is mainly caused by the high frequency region. So $LiFe_{0.98}Nb_{0.02}PO_4/C$ impedance is the smallest. Compared to other samples, it is easier to overcome the constraints of dynamic charge and more conducive to Li^+ de-embedding. At the same time, electrochemical performance is better.
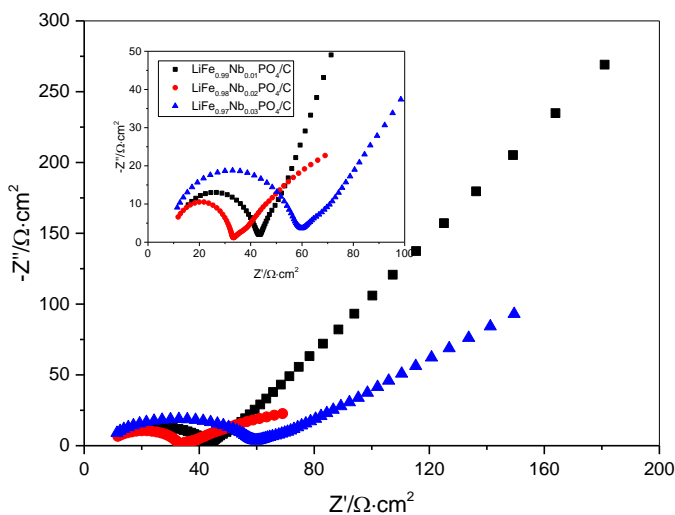

Figure 6. AC impedance of $LiFe_{1-x}Nb_xPO_4/C$ (x=0.01, 0.02, 0.03)

4. CONCLUSIONS

XRD results showed that doping Nb^{5+} into the $LiFePO_4/C$ changed the lattice constant, but did not change the crystal form of $LiFePO_4$. Physical morphology had also been greatly changed. Particle size is smaller and more uniform.

Through a series of electrical performance tests, it was found that when the Nb^{5+} doping amount was 0.02, the charge-discharge specific capacity of the material decreased with the increase of doping amount. In addition, the doped material had better high-rate performance and less attenuation.

The results of cyclic voltammetry showed that there were four pairs of redox peaks in the curve, which were consistent with the peaks on the charge-discharge curve. When the doping amount was 0.02, the cyclic voltammetry peak was high. So the material had the best performance when the doping amount was 0.02.

References

1. X.B. Meng, X.Q. Yang, X.L. Sun, *Advanced Materials,* 24 (2012) 3589.

2. T.F. Yi, X.Y. Li, H.P. Liu, *Ionic*s, 18 (2012) 529.
3. B. Wang, Al. Abdulla. W, D. Wang, *Energy & Environmental Science,* 8 (2015) 869.
4. P. Hovington, M. Lagacé, A. Guerfi, *Nano Letters,* 15 (2015) 2671.
5. M. Shi, L.B. Kong, J. B, Ionics, 22 (2016) 185.
6. Y. Xu, J. Mao, *Journal of Materials Science,* 51 (2016) 10026.
7. J. Song, B. Sun, H. Liu, *ACS Applied Materials & Interfaces,* 8 (2016) 15225.
8. O.Y. Posudievsky, O.A. Kozarenko, V.S. Dyadyun, *Journal of Solid State Electrochemistry,* 19 (2015) 2733.
9. A. Chekannikov, S. Novikova, T. Kulova, *Journal of Electrochemical Science And Engineering,* 6 (2016) 1.
10. A. Örnek, O. Efe, *Electrochimica Acta,* 166 (2015) 338.
11. X. Zhang, M.V. Hulzen, D.P. Singh, *Nature Communications,* 6 (2015)1.
12. Y. Yang, K. Li, H. Li, *International Journal of Applied Ceramic Technology,* 12 (2015) 163.
13. V. Timoshevskii, Z. Feng, K.H. Bevan, *ACS Applied Materials & Interfaces,* 7 (2015) 18362.
14. W. Su, K. Xu, G. Zhong, *International Journal of Electrochemical Science,* 12 (2017) 6930.
15. Y. Ding, P. Pan, L.H. Chen, Z.B. Fu, J. Du, L.G. Guo and F. Wang, *Ionics,* 1 (2017) 1.
16. B. Zhang, X. Yuan, H. Li, X. Wang, J. Zhang, H. Chen and J. Zheng, *Journal of Alloys and Compounds,* 627 (2014) 13.
17. L. Qu, D. Luo, S. Fang, Y. Liu, L. Yang, S.I. Hirano and C.C. Yang, *Journal of Power Sources,* 307 (2016) 69.
18. Z.C. Shao, J.L Xia, X.Q. Liu and G.Y. Li, *Materials and Manufacturing Processes,* 31 (2015) 695.
19. X. Meng, B. Han, Y.F. Wang, J.Y. Nan, *Ceramics International,* 42 (2015) 2599.
20. P.P. Sun, H.Y. Zhang, K. Shen, Q. Fan, and Q.Y. Xu, *Journal of Nanoscience and Nanotechnology,* 15 (2015) 2667.
21. J.S. Huang, L. Yang, K.Y. Liu, Y.F. Tang, *Journal of Power Sources,* 195 (2010) 5013.
22. X.J. Yang, Z.D. Hu, J. Liang, *Ceramics International,* 41 (2015) 2863.